Characteristics of the rotor R4-06 for the O4 NCal system VIR-0860A-22

Eddy Dangelser, Dimitri Estevez, Benoit Mours,
Mehmet Ozturk, Antoine Syx

IPHC-Strasbourg

September 8, 2022

Contents

1 Introduction

This note follows the same discussion made on the rotor R4-01 in VIR-0591C-22 and R4-05 in VIR-0859A-22. The drawings and figures of the rotor can be found in this first technical note.

The rotor has been engraved IPHC-R4-06 on one side and sandblasted on the other side.

2 Measurement method

To determine the geometry of the rotor we will use the same method as for R4-01 (see VIR-0591C-22). The thickness was measured using 24*2 = 48 points (see fig. 1), the outer diameter was measured in 4*2 = 8 points and the inner diameter using 4 points.

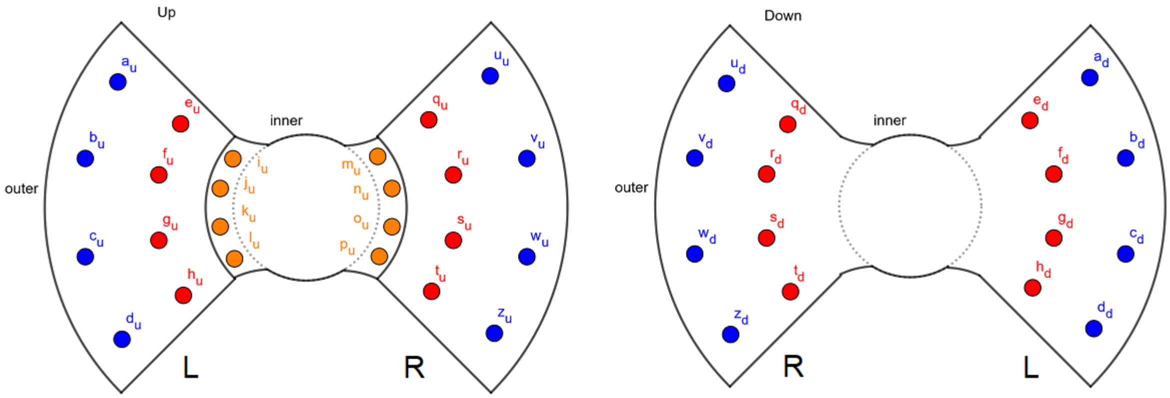

Figure 1: Outline of the faces of the rotor with the measurement points. Left figure is face up, right figure is face down. Sectors have been labelled L for left sector and R for right sector.

The tool used to measure the thickness and the outer diameter is a measuring column "Garant 44 5350_600 HC1" (see VIR-0160A-22) with a given precision of 1.8+L/600 μm (L the measured length in mm). A vernier caliper "TESA-CAL IP67" with a precision of 20 μm was used to measure the inner diameter.

The measuring column was operated on a metrology table with a value range from 0 to 2 μm. The rms of the 16 values is 0.9 μm.

We measured the opening angles of the sectors using a video measuring microscope "Garant MM2" (see VIR-0591C-22) with a given precision of 2.9+L/100 μm at 95% CL (L the measured length in mm).

2.1 Thermal effects and density

The rotor R4-06 has been machined from the same aluminum block as R4-05 described in VIR-0859A-22. As for R4-05 the results will be expressed at a reference temperature of 23°C.

The density of the rotor R4-06 is then 2810.8 $\pm$ 0.2 kg.m^{-3}. This density is measured in air, if the rotor is used under vacuum, the density should be increased by the air density (ρ_{air}=1.3 kg.m^{-3}).

3 Raw measurements of the rotor

This section presents the raw measurements made on the rotor at the ambient temperature of 24.4°C. Table 1 shows the thickness measurements according to the measurement points defined in figure 1. The rotor is laying on the table. The rotor surface as well as the table are not perfectly flat. Some space could be present in between that should be substracted when computing the rotor thickness as discussed later.

Measurement point	L sector		Measurement point	R sector	
	Up	Down		Up	Down
a	104.405	104.401	q	104.368	104.371
b	104.417	104.414	r	104.364	104.369
c	104.419	104.421	s	104.366	104.373
d	104.413	104.417	t	104.375	104.377
e	104.411	104.410	u	104.333	104.332
f	104.413	104.413	v	104.335	104.332
g	104.415	104.416	w	104.340	104.334
h	104.416	104.416	z	104.343	104.345
i	101.489		m	101.490	
j	101.487		n	101.490	
k	101.488		o	101.490	
l	101.492		p	101.493	

Table 1: Raw measurements of the height in mm for each point at 24.4°C on L and R sectors of R4-06.

Table 2 displays the diameter measurements. The measurements were made on 4*2 diameters (two parts of each diameter, the up and down sides of the rotor).

Measurement point	Up	Down
1	207.942	207.939
2	207.973	207.967
3	207.976	207.980
4	207.933	207.960

Table 2: Raw measurements of the diameter in mm for each point at 24.4°C on R4-06.

Theoretical values were taken for the inner radius r_{min} = 29 mm and the up face radius for the counterweight $r_{\text{counterweight}}$ = 40 mm (see drawing in VIR-0591C-22).

4 Extracting the geometrical parameters

4.1 Thickness

We need to correct the possible gap between the rotor and the measuring table. Assuming that the table is flatter than the rotor surface we can extract the gap from the measurement of the top surface considering the plane tangents to the highest points (asking them to be on both sectors). For this rotor these points are b, c, t for the up and c, d, t for the down face (see fig. 1). Using the measurements in table 1 we can compute a plane equation for each side of the rotor in cartesian coordinates:

$$\text{Up plane equation}: z = -3.38 \times 10^{-4}x - 5.92 \times 10^{-5}y + 104.39 \tag{1}$$

$$\text{Down plane equation : } z = -3.32 \times 10^{-4}x - 1.24 \times 10^{-5}y + 104.39 \tag{2}$$

Using eqs. (1) and (2) the gap can be determined, see table 3. The maximum rms of the gap for each sector is 13 μm.

Measurement point	L sector		Measurement point	R sector	
	Up	Down		Up	Down
a	6	15	q	3	5
b	0	7	r	6	5
c	0	0	s	5	1
d	3	0	t	0	0
e	-8	-3	u	28	35
f	-6	-3	v	24	31
g	-7	-5	w	21	30
h	-10	-8	z	24	24

Table 3: Gap computed in μm on up and down sides of both sectors of R4-06.

We can then compute the rotor thickness for each point by removing these gaps. If one of the raw values is lower than the corrected thickness we take this lowest value. The value of each point is shown in table 4 at 23°C.

Measurement point	L sector	Measurement point	R sector
a	104.398	q	104.365
b	104.410	r	104.361
c	104.416	s	104.363
d	104.410	t	104.372
e	104.398	u	104.329
f	104.403	v	104.329
g	104.406	w	104.331
h	104.403	z	104.340
i	101.486	m	101.487
j	101.484	n	101.487
k	101.485	o	101.487
l	101.489	p	101.490

Table 4: Measurements of the thickness in mm for each point at 23°C on L and R sectors of R4-06.

4.2 Radius

Using comparators while the rotor is rotating on its axis we can determine the deformation on both sectors and compute different radii values. Table 5 shows the raw measurements using comparators on L and R sectors. The measurements were made on the up, center and down sides of L and R sectors using three comparators for a total of 5*3*2=30 points (the first and last points are near the edge of the sectors).

Measurement point	L sector			R sector		
	Up	Center	Down	Up	Center	Down
A	-10	50	0	-5	5	-5
B	35	45	35	30	45	35
C	40	50	40	35	45	40
D	30	45	30	20	30	30
E	0	0	0	-25	-5	-5

Table 5: Raw measurements in μm of the comparators for the L and R sectors of R4-06.

The zeroing of the comparators was made arbitrarily close to the edge of the sector. The offsets shown in table 5 are measured relative to this reference.

To compute the radius per measurement point we use the following process: First we compute the mean deformation for one comparator. Then we remove this mean deformation to each measurement of this comparator. The corrected shift value is added to the mean radius of 103.976 mm computed using table 2 at 23°C. This process is repeated for each comparator. The final radius for each point are shown in table 6.

Measurement point	L sector			R sector		
	Up	Center	Down	Up	Center	Down
A	103.954	103.998	103.959	103.959	103.953	103.954
B	103.999	103.993	103.994	103.994	103.993	103.994
C	104.004	103.998	103.999	103.999	103.993	103.999
D	103.994	103.993	103.989	103.984	103.978	103.989
E	103.964	103.948	103.959	103.939	103.943	103.954

Table 6: Radius measurements in mm at 24.4°C for the L and R sectors of R4-06.

5 Characterization of the rotor using a simple model

5.1 Theoretical model of the rotor

As explained in VIR-0591C-22 the theoretical strain of the mirror at 2f using FROMAGE v1r2 with the rotor design parameters:

$$\text{strain(2f)} = \frac{2.1217 \times 10^{-18}}{(2f_{rot})^2}$$

This strain value will be compared to models based on the measurements of the rotor.

5.2 Thickness

A simple model can be used to determine a mean value for the thickness and its uncertainty.

As shown on fig. 1, a total of 16 points were used to compute the thickness of each sector. In this case we will not consider the inner points so that we obtain uniform sectors.

For the simple model we take the thickness as the mean value of table 4: 104.377 mm at 23°C. Since we have a limited number of measurement points, to be conservative we take the thickness uncertainty as the rms of table 4 (32.3 μm) to which we add linearly the metrology table uncertainty (0.9 μm) and the tool uncertainty (2.0 μm). Therefore, for this simple model, the thickness is 104.377 ± 0.035 mm.

5.3 Radius

For the simple model we take the radius as the mean value of table 6: 103.976 mm at 23°C. Using a linear sum of the rms of table 6 (20.8 μm) and the tool uncertainty (2.2 μm) we take an uncertainty of 23 μm on the mean radius.

We have to point out that we do not take into account the fact that the sectors might not be centered on the same axis. Therefore the uncertainty might be underestimated. We will then consider each sector individually later.

5.4 Expected NCal signal and uncertainties

The geometry used to describe the rotor as a simple model is represented in figure 2.

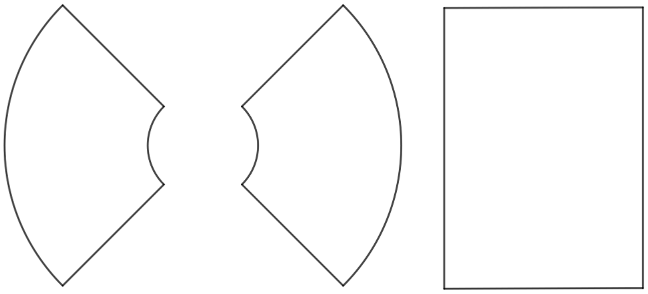

Figure 2: Simple model geometry used to describe the rotor. Left is a front view, right is a side view.

Using the analytical equation of the strain at 2f (see eq.8 in Newtonian calibrator tests during the Virgo O3 data taking) we compute with our parameters (d = 1.7 m and an angle ϕ = 34.7°):

$$\text{strain(2f)} = \frac{2.1193 \times 10^{-18}}{(2f_{rot})^2}.$$

Using FROMAGE on this geometry we compute the following 2f strain on the mirror at a distance of 1.7m and an angle of 34.7°:

$$\text{strain(2f)} = \frac{2.1194 \times 10^{-18}}{(2f_{rot})^2}$$

Comparing the theoretical model strain with the simple model at 2f using FROMAGE we obtain a relative deviation of 0.108%.

Comparing the analytical strain at 2f with FROMAGE we obtain a relative deviation of 0.005%.

The uncertainties considered for this model are displayed in table 7.

R4-06 rotor parameter simple model (23°C)			NCal 2f signal uncertainty	
name	value	uncertainty	formula	value (%)
Density ρ (kg.m^{-3})	2810.8	0.2	$\delta\rho/\rho$	0.007
Thickness b (mm)	104.377	3.5×10^{-2}	$\delta b/b$	0.034
r_{max} (mm)	103.976	2.3×10^{-2}	$4\delta r_{max}/r_{max}$	0.088
G (m^3.kg^{-1}.s^{-2})	$6.674\,30 \times 10^{-11}$	1.5×10^{-15}	$\delta G/G$	0.002
Temperature T (°C)	23	3	$\left\lvert\frac{\partial h}{\partial T}\right\rvert \frac{\Delta T}{h}$	0.014
Quadratic sum				0.096

Table 7: Uncertainties on the amplitude of the calibration signal at 2f from the R4-06 rotor simple model geometry.

6 Characterization of the rotor using an advanced model

6.1 Thickness

A more advanced model can be used considering the deformations on the surfaces of the sectors for better accuracy. Each measurement point of table 4 can be considered as a sub-sector with its own thickness.

The uncertainty on this value is more complex to evaluate. As a conservative approach we use the maximum rms of the deviation to a plane for each sector (13 μm see section 4.1) to which we add linearly the uncertainty on the flatness of the measurement table (0.9 μm) as well as the measurement tool (2.0 μm). The total uncertainty on the thickness is 16 μm.

6.2 Radius

On fig. 1 we divided the external sectors in 4 sub-sectors for each sector (blue points). We convert the point of table 6 to the grid of fig. 1 by averaging the two closest values and converting them to 23°C. The results are shown in table 8. We notice that the L sector is on average 7 μm larger than the R sector.

Radius	L sector			R sector		
	Up	Center	Down	Up	Center	Down
1	103.973	103.992	103.973	103.973	103.970	103.971
2	103.998	103.992	103.993	103.993	103.990	103.993
3	103.996	103.992	103.991	103.988	103.982	103.991
4	103.976	103.967	103.971	103.958	103.957	103.968

Table 8: Radius measurements (in mm at 23°C) for the L and R sectors of R4-06.

The maximum rms of the radii for each sector is 13.3 μm. The tool uncertainty is 2.2 μm. Like for the thickness we use a linear sum and find the uncertainty on both radii to be 16 μm.

6.3 Counterweight

To balance this rotor, two masses m_1 and m_2 were respectively placed at angles α_1 and α_2 and at a radius r_m. Using the following formula we can compute a single mass equivalent to the moment of the two masses:

$$m = \sqrt{m_1^2 + m_2^2 + 2m_1 m_2 \cos(\alpha_1 - \alpha_2)} \tag{3}$$

Using the result of eq. (3) and the following formulas (where ρ_{Al} is the density of the aluminum counterweight, h its thickness and R its outer radius) we can compute the angle of the chord cut (γ_m) on the counterweight and its position angle (α_m):

$$\gamma_m = \arcsin\left[\left(\frac{3}{2}\frac{m\ r_m}{\rho_{\mathrm{Al}}\ h\ R^3}\right)^{1/3}\right] \tag{4}$$

$$\alpha_m = \arctan\frac{m_1\sin(\alpha_1) + m_2\sin(\alpha_2)}{m_1\cos(\alpha_1) + m_2\cos(\alpha_2)} \tag{5}$$

A counterweight has been designed to reduce the unbalance of the rotor. This counterweight is made of aluminum 2017 ($\rho_{\mathrm{Al}_{2017}} = 2790$ kg.m^{-3}) and the geometry is shown in fig. 3.

The dimensions of the counterweight are: an inner radius of 10 mm, an outer radius of 40 mm and a material cut with a chord of 70.07 mm to balance the rotor (see hatched are on fig. 3).

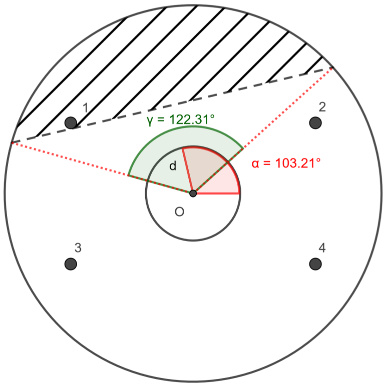

Figure 3: Outline of the counterweight for R4-06. The hatched area represents the material removed.

6.4 Opening angles and asymmetry

The opening angles of the full and empty sectors have been measured using a video microscope with the same method as for R4-01. The uncertainty on α = 0.2 mrad is the same as for R4-01 giving an uncertainty of 4×10^{-6} % on the 2f signal which is neglectable.

The measurements are shown in table 9. The center value corresponds to the mean of up and down measurements.

Opening angle	Up	Center	Down
L	1.57072	1.57091	1.57109
R	1.57092	1.57091	1.57091
L-R	1.57088	1.57085	1.57083
R-L	1.57066	1.57051	1.57036

Table 9: Opening angle measurements in rad for the L, R full sectors and L-R, R-L empty sectors of R4-06.

These measurements allow us to compute the signal with different opening angles and an asymmetry between the sectors. These measured opening angles will be included in the advanced model described in the next section.

6.5 Expected NCal signals and uncertainties

6.5.1 Advanced geometry including chamfers and counterweight

The geometry used to describe the rotor as an advanced model is represented in figure 4. The external parts of the sectors are divided in 3 sub-sectors each to correspond to the different radii determined. In addition we include the counterweight, the screws, the screw holes, the opening angles and asymmetry of the sectors.

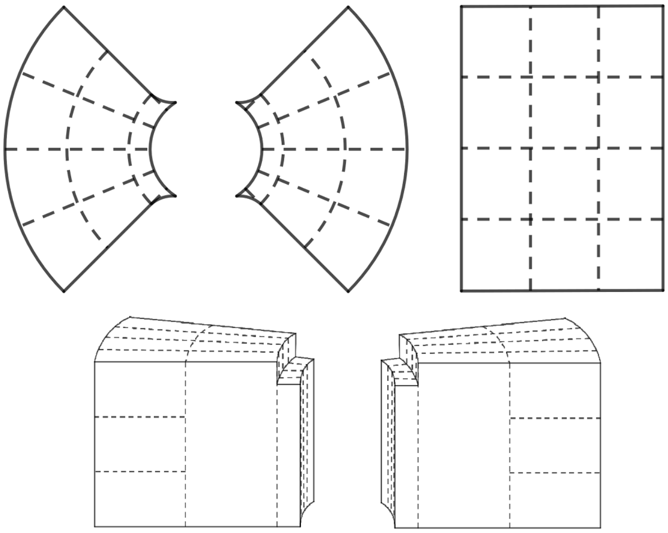

Figure 4: Advanced model geometry used to describe the rotor. Top left is a front view, top right is a side view (external sub-sectors) and bottom is a tilted view of the sectors. Only the 4 external part sectors are divided in 3 sub-sectors each. The chamfers are visible on the inner radius.

Using FROMAGE on this geometry gives the following strains:

- strain(1f) = $\dfrac{3.1823 \times 10^{-20}}{(1 f_{rot})^2}$
- strain(2f) = $\dfrac{2.1194 \times 10^{-18}}{(2 f_{rot})^2}$
- strain(3f) = $\dfrac{3.9677 \times 10^{-23}}{(3 f_{rot})^2}$

The relative deviation to the simple model at 2f is 0.005%.

6.5.2 Remaining geometry uncertainty

Since R4-02 and following have been machined with a better precision than R4-01 as seen from the lower 1f value. The remaining geometry uncertainties are taking as for R4-01.

6.5.3 Uncertainties

To set an uncertainty on the strain(2f) from the description of the geometry we take the difference between the simple model (strain(2f) = $2.1194 \times 10^{-18}/(2f)^2$) and the advanced model (strain(2f) = $2.1195 \times 10^{-18}/(2f)^2$). This deviation, 0.005%, is reported in table 10 as modelling uncertainty.

The uncertainties considered for this full model are displayed in table 10.

R4-06 rotor parameter advanced model (23°C)			NCal 2f signal uncertainty	
name	mean value	uncertainty	formula	value (%)
Density ρ (kg.m^{-3})	2810.8	0.2	$\delta\rho/\rho$	0.007
Thickness b left sector (12 sub-sectors) (mm)	104.405	1.6×10^{-2}	$\delta b/b$	0.015
Thickness b right sector (12 sub-sectors) (mm)	104.348			
r_{max} left sector (12 ext sub-sectors) (mm)	103.985	1.4×10^{-2}	$4\delta r_{max}/r_{max}$	0.059
r_{max} right sector (12 ext sub-sectors) (mm)	103.978			
G (m^3.kg^{-1}.s^{-2})	$6.674\,30 \times 10^{-11}$	1.5×10^{-15}	$\delta G/G$	0.002
Temperature T (°C)	23	3	$\left\lvert\frac{\partial h}{\partial T}\right\rvert \frac{\Delta T}{h}$	0.014
Modelling Uncertainty				0.005
FROMAGE grid uncertainty				0.005
Opening angle and sector asymmetry uncertainty				$<5 \times 10^{-4}$
Remaining geometry uncertainty				$<5 \times 10^{-4}$
Total uncertainty from the rotor (quadratic sum)				0.064

Table 10: Uncertainties on the amplitude of the calibration signal at 2f from the R4-06 rotor advanced model geometry at 23°C.

A Appendix

```
### This is a cfg file for a more realistic geometry of the mirror and the Virgo NCal R4-06 (2022)

### ALL THE OBJECTS ARE DEFINED IN THE MIRROR’S FRAME (O,x,y,z),
### with O the center of the mirror, x axis along the ITF’s beam toward the beam-splitter,
### y axis orthogonal to x in the plane of the ITF,
### z axis orthogonal to the plane of the ITF upward

### MIRROR DEFINITION

GRID_SIZE 12 30 8

CYLINDER 2202. 0 0.175 0.2 360 0 0 0

GRID_SIZE 1 1 1

# Defining the flats on the edge of the mirror
CUT_CYL 2202. 0.175 0.2 0.05 0 0
CUT_CYL 2202. 0.175 0.2 0.05 0 180

# Defining the ears and anchors of the mirror
CUBOID 2202. 0.090 0.010 0.015  0     0.1782 -0.0125
CUBOID 2202. 0.090 0.010 0.015  0    -0.1782 -0.0125
CUBOID 2202. 0.039 0.008 0.008 -0.02 -0.1772 -0.024
CUBOID 2202. 0.039 0.008 0.008 -0.02  0.1772 -0.024
CUBOID 2202. 0.039 0.008 0.008  0.02 -0.1772 -0.024
CUBOID 2202. 0.039 0.008 0.008  0.02  0.1772 -0.024

### ROTOR DEFINITION: CYLINDER DENSITY INNER_RADIUS OUTER_RADIUS THICKNESS OPEN_ANGLE r z theta

ROTOR_CYLINDRICAL 1.7 34.7 0 0

### COUNTERWEIGHT 2790.
GRID_SIZE 16 65 40
CYLINDER 2790. 0.010 0.040 0.003 360 0 0.049513 0
GRID_SIZE 1 1 1
CUT_CYL 2790. 0.040 0.003 0.07007 0 103.21

### SCREW HOLES
GRID_SIZE 4 4 4
CYLINDER -2810.8 0 0.0015 0.012 360 0.03 0.04474282340172 150
CYLINDER -2810.8 0 0.0015 0.012 360 0.03 0.04474432335216 30
CYLINDER -2810.8 0 0.0015 0.012 360 0.03 0.0447433233852 210
CYLINDER -2810.8 0 0.0015 0.012 360 0.03 0.04474482333564 330

### SCREWS COUNTERWEIGHT
CYLINDER 4810. 0 0.0015 0.003 360 0.03 0.0493696683339 150
CYLINDER 7600. 0 0.0015 0.00665 360 0.03 0.04409482333564 150

CYLINDER 4810. 0 0.0015 0.003 360 0.03 0.0493696683339 30
CYLINDER 7600. 0 0.0015 0.00665 360 0.03 0.04409482333564 30

CYLINDER 4810. 0 0.0015 0.003 360 0.03 0.0493696683339 210
CYLINDER 7600. 0 0.0015 0.00665 360 0.03 0.04409482333564 210
```

```
CYLINDER 4810. 0 0.0015 0.003 360 0.03 0.0493696683339 330
CYLINDER 7600. 0 0.0015 0.00665 360 0.03 0.04409482333564 330

# TRES RAPIDE
#GRID_SIZE 4 4 4
# RAPIDE
#GRID_SIZE 8 17 14
# LENT
GRID_SIZE 8 65 40

### L sector

## Inner part
OUTER_FILLET 2810.8 0.029 0.101486 -0.002917 0.01 -11.25 146.2477
CYLINDER 2810.8 0.029 0.04 0.101486 22.5 0 -0.002917 146.2477
CYLINDER 2810.8 0.029 0.04 0.101484 22.5 0 -0.002919 168.7492
CYLINDER 2810.8 0.029 0.04 0.101485 22.5 0 -0.002917 191.2508
CYLINDER 2810.8 0.029 0.04 0.101489 22.5 0 -0.002917 213.7523
OUTER_FILLET 2810.8 0.029 0.101489 -0.002917 0.01 11.25 213.7523

## Middle part
CYLINDER 2810.8 0.04 0.071998 0.104398 22.5 0 0 146.2477
CYLINDER 2810.8 0.04 0.071998 0.104403 22.5 0 0 168.7492
CYLINDER 2810.8 0.04 0.071998 0.104406 22.5 0 0 191.2508
CYLINDER 2810.8 0.04 0.071998 0.104403 22.5 0 0 213.7523

## Outer part
CYLINDER 2810.8 0.071998 0.103973 0.03479918353032 22.5 0 0.03479918353032 146.2516
CYLINDER 2810.8 0.071998 0.103992 0.03479918353032 22.5 0 0 146.2477
CYLINDER 2810.8 0.071998 0.103973 0.03479918353032 22.5 0 -0.03479918353032 146.2438

CYLINDER 2810.8 0.071998 0.103998 0.0348034864751664 22.5 0 0.0348034864751664 168.7505
CYLINDER 2810.8 0.071998 0.103992 0.0348034864751664 22.5 0 0 168.7492
CYLINDER 2810.8 0.071998 0.103993 0.0348034864751664 22.5 0 -0.0348034864751664 168.7479

CYLINDER 2810.8 0.071998 0.103996 0.03480518333208 22.5 0 0.03480518333208 191.2495
CYLINDER 2810.8 0.071998 0.103992 0.03480518333208 22.5 0 0 191.2508
CYLINDER 2810.8 0.071998 0.103991 0.03480518333208 22.5 0 -0.03480518333208 191.2521

CYLINDER 2810.8 0.071998 0.103976 0.03480318339816 22.5 0 0.03480318339816 213.7484
CYLINDER 2810.8 0.071998 0.103967 0.03480318339816 22.5 0 0 213.7523
CYLINDER 2810.8 0.071998 0.103971 0.03480318339816 22.5 0 -0.03480318339816 213.7562

### R sector

## Inner part
OUTER_FILLET 2810.8 0.029 0.101487 -0.002878 0.01 11.25 33.7427
CYLINDER 2810.8 0.029 0.04 0.101487 22.5 0 -0.002878 33.7427
CYLINDER 2810.8 0.029 0.04 0.101487 22.5 0 -0.002878 11.2410
CYLINDER 2810.8 0.029 0.04 0.101487 22.5 0 -0.002878 348.7394
CYLINDER 2810.8 0.029 0.04 0.101490 22.5 0 -0.002875 326.2377
OUTER_FILLET 2810.8 0.029 0.101490 -0.002875 0.01 -11.25 326.2377

## Middle part
CYLINDER 2810.8 0.04 0.071998 0.104365 22.5 0 0 33.7427
CYLINDER 2810.8 0.04 0.071998 0.104361 22.5 0 0 11.2410
```

```
CYLINDER 2810.8 0.04 0.071998 0.104363 22.5 0 0 348.7394
CYLINDER 2810.8 0.04 0.071998 0.104372 22.5 0 0 326.2377

## Outer part
CYLINDER 2810.8 0.071998 0.103973 0.03477618429024 22.5 0 0.03477618429024 33.7428
CYLINDER 2810.8 0.071998 0.103970 0.03477618429024 22.5 0 0 33.7427
CYLINDER 2810.8 0.071998 0.103971 0.03477618429024 22.5 0 -0.03477618429024 33.7426

CYLINDER 2810.8 0.071998 0.103993 0.03477618429024 22.5 0 0.03477618429024 11.2411
CYLINDER 2810.8 0.071998 0.103990 0.03477618429024 22.5 0 0 11.2410
CYLINDER 2810.8 0.071998 0.103993 0.03477618429024 22.5 0 -0.03477618429024 11.2410

CYLINDER 2810.8 0.071998 0.103988 0.03477685093488 22.5 0 0.03477685093488 348.7393
CYLINDER 2810.8 0.071998 0.103982 0.03477685093488 22.5 0 0 348.7394
CYLINDER 2810.8 0.071998 0.103991 0.03477685093488 22.5 0 -0.03477685093488 348.7394

CYLINDER 2810.8 0.071998 0.103958 0.03477985083576 22.5 0 0.03477985083576 326.2376
CYLINDER 2810.8 0.071998 0.103957 0.03477985083576 22.5 0 0 326.2377
CYLINDER 2810.8 0.071998 0.103968 0.03477985083576 22.5 0 -0.03477985083576 326.2378

### GENERAL PARAMETERS

STEP 22.5 16

ARM_LENGTH 3000

SIGNAL 3
```